Research Square

Preprints are preliminary reports that have not undergone peer review.
They should not be considered conclusive, used to inform clinical practice,
or referenced by the media as validated information.

Spirulina platensis Polysaccharides: Evaluation of Immunomodulatory Activity and Mechanism via NF-κB Signaling Pathway Activation in RAW264.7 Cells

Li-Chao Pan
Lanzhou University of Technology
Wen-Hui Zhang
Lanzhou University of Technology
Juan Li
Lanzhou University of Technology
Ruo-Bing Wu
Lanzhou University of Technology
Tong-Yao Niu
Lanzhou University of Technology
Shu-Min Song
Gansu Zhongqing Light Industry Product Quality Inspection Co.,Ltd.
Sheng-Hui Yang
Gansu Kaiyuan Biotechnology Development Center Co., Ltd.
Guang-Hong Luo
Gansu Kaiyuan Biotechnology Development Center Co., Ltd.
Hai-Wei Ren
rhw525711190163.com

Lanzhou University of Technology

Research Article

Keywords: Spirulina platensis, polysaccharide, RAW264.7 macrophages, immunomodulation, NF-κB signaling

Posted Date: November 11th, 2026

DOI: https://doi.org/10.21203/rs.3.rs-11399583/v1

License: This work is licensed under a Creative Commons Attribution 4.0 International License.
Read Full License

Additional Declarations: No competing interests reported.

Spirulina platensis Polysaccharides: Evaluation of Immunomodulatory Activity and Mechanism via NF-κB Signaling Pathway Activation in RAW264.7 Cells

Li-Chao Pan[1,2,3,†], Wen-Hui Zhang[1,†], Juan Li[1], Ruo-Bing Wu[1], Tong-Yao Niu[1], Shu-Min Song[4], Sheng-Hui Yang[2,3], Guang-Hong Luo[2,3], Hai-Wei Ren[1*]

[1]*School of Life Science and Engineering, Lanzhou University of Technology, Lanzhou 730050, China*

[2]*Gansu Kaiyuan Biotechnology Development Center Co., Ltd., Zhangye 734000, China*

[3]*Microalgae Technology Innovation Center of Gansu Province, Hexi University, Zhangye 734000, China*

[4]*Gansu Zhongqing Light Industry Product Quality Inspection Co.,Ltd., Lanzhou 730030, China*

[*] ***Corresponding author.*** *E-mail:* rhw52571119@163.com *(Hai-Wei Ren)*

[†]*These authors contributed equally to this work.*

Declarations

Funding

This work was supported by the Postdoctoral Project of Gansu Kaiyuan Biotechnology Development Center Co., Ltd. (24KYBH001) and the Intellectual Property Plan—Intellectual Property Protection Project (25ZSCQG024).

Competing interests

All authors declare that they have no competing financial interests or personal relationships.

Availability of data and material

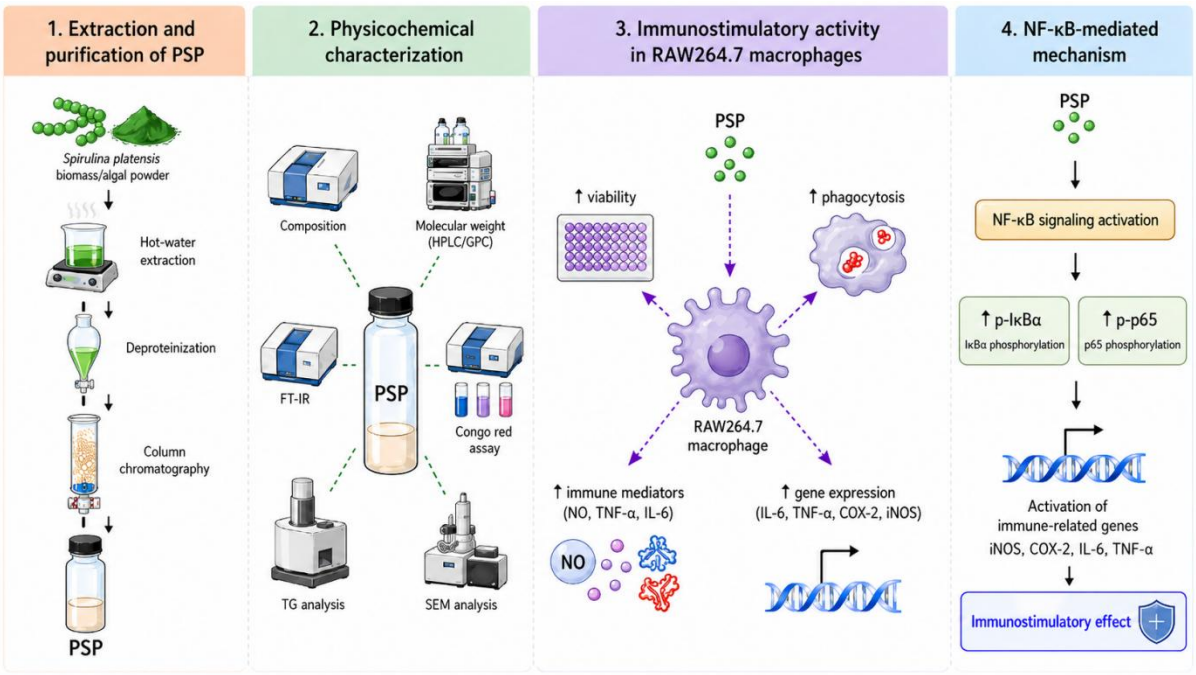
The data generated or analyzed during this study are available from the corresponding author on reasonable request.

Code availability

Not applicable

Authors' contributions

Li-Chao Pan: Conceptualization, supervision, writing—review and editing. Wen-Hui Zhang: Data curation, writing—original draft, writing—review and editing. Juan Li: Data curation, writing—review and editing. Ruo-Bing Wu: Methodology, data curation. Tong-Yao Niu: Investigation, formal analysis. Shu-Min Song: Methodology, investigation, validation. Sheng-Hui Yang: Investigation, formal analysis. Guang-Hong Luo: Funding acquisition, investigation, methodology, project administration, resources, supervision. Hai-Wei Ren: Conceptualization, funding acquisition, methodology, project administration, supervision. All authors read and approved the final manuscript.



Graphical Abstract

Abstract

A high-molecular-weight polysaccharide (PSP; 2.54 × 10^6 Da) was isolated from *Spirulina platensis* and characterized. PSP consisted of mannose, rhamnose, glucose, galactose, xylose, and arabinose at a molar ratio of 36.32:33.24:20.83:4.52:2.84:2.26. Structural analyses showed that PSP adopted a helical conformation, exhibited a sheet-like morphology, and remained thermally stable below 230 °C. At non-cytotoxic concentrations, PSP significantly enhanced phagocytic activity and nitric oxide (NO) production in RAW264.7 macrophages. PSP also increased the secretion of tumor necrosis factor-α (TNF-α) and interleukin-6 (IL-6), together with the messenger RNA expression of inducible nitric oxide synthase (iNOS), cyclooxygenase-2 (COX-2), TNF-α, and IL-6. The strongest responses were generally observed at lower PSP concentrations, whereas the effects decreased as the concentration increased. Western blot analysis demonstrated increased phosphorylation of inhibitor of nuclear factor kappa B alpha (IκBα) and p65 after PSP treatment. Mechanistic analyses further indicated that PSP activated nuclear factor kappa B (NF-κB) signaling, suggesting that NF-κB activation contributed to PSP-mediated macrophage stimulation. Collectively, these findings establish PSP as a bioactive Arthrospira-derived macromolecular polysaccharide with marked in vitro immunomodulatory activity and support its potential development as a natural immunomodulatory agent.

Keywords: *Spirulina platensis*; polysaccharide; RAW264.7 macrophages; immunomodulation; NF-κB signaling

1 Introduction

The immune system consists of both innate immunity and adaptive immunity and plays an important role in defending against pathogen infection, eliminating abnormal cells, and maintaining homeostasis (Soares et al. 2017; Rankin and Artis 2018). Innate immunity serves as the first line of defense against external stimuli. It recognizes pathogen-associated molecular patterns through pattern recognition receptors (PRRs) and induces corresponding defense responses in immune cells (Rivera et al. 2016). Macrophages are important effector cells of the innate immune system and are widely distributed in different tissues. They participate in

antigen recognition, phagocytic clearance, and the release of inflammatory mediators. Upon stimulation, macrophages can be activated and initiate multiple intracellular signaling pathways, thereby regulating immune responses (Franken et al. 2016; Christofides et al. 2022).

Spirulina platensis is a cyanobacterial microorganism with high nutritional value. Because of its high protein content and various functional components, it has been widely used in foods, nutritional supplements, and functional food products (Podgórska-Kryszczuk 2024; Marjanović et al. 2024). In addition to proteins, carotenoids, and polyunsaturated fatty acids, *Spirulina platensis* is also rich in extracellular and intracellular polysaccharides with diverse biological activities (Spínola et al. 2024). In recent years, *Spirulina platensis* polysaccharides (PSP) have attracted considerable attention because of their good biocompatibility, safety, and potential health-promoting effects (Fratelli et al. 2021; Cai et al. 2022; Ai et al. 2023). Previous studies have shown that PSP possesses antioxidant (Liao et al. 2023), immunomodulatory (Hamedifard et al. 2019), and antitumor activities (Yu et al. 2018). These biological functions are closely related to their molecular weight, monosaccharide composition, glycosidic linkages, and spatial conformation (Patel et al. 2023; Fu et al. 2024). In terms of immunomodulation, PSP can interact with pattern recognition receptors on the surface of immune cells, regulate the functions of macrophages and lymphocytes, and promote the release of immune mediators, thereby enhancing nonspecific immune defense (Yin et al. 2019; Li et al. 2023; Yi et al. 2025). However, the molecular mechanisms by which PSP promotes macrophage activation have not been fully clarified, especially whether it regulates immune effector functions through key inflammatory signaling pathways.

Macrophage activation involves several complex intracellular signaling pathways, among which the nuclear factor-kappa B (NF-κB) signaling pathway is an important regulator of inflammatory responses and immune functions (Dorrington and Fraser 2019). Under resting conditions, NF-κB is usually bound to its inhibitory protein IκB and retained in the cytoplasm. When cells are stimulated by lipopolysaccharide (LPS) or other immune stimuli, the IκB kinase (IKK) complex is activated, leading to the phosphorylation and degradation of IκBα. This process releases the NF-κB dimer, allowing it to translocate into the nucleus and bind to the promoter regions of target genes, thereby regulating the expression of immune-related genes

(Barnabei et al. 2021; Mussbacher et al. 2023). Activation of NF-κB can induce the transcription of several inflammation- and immunity-related genes, including inducible nitric oxide synthase (iNOS), cyclooxygenase-2 (COX-2), tumor necrosis factor-α (TNF-α), and interleukin-6 (IL-6) (Liu et al. 2017; Oeckinghaus et al. 2011; Wang et al. 2025). Nitric oxide (NO) produced by iNOS, together with inflammatory cytokines, contributes to pathogen clearance, immune cell recruitment, and host defense (Yang et al. 2023; Park et al. 2022). However, sustained or excessive activation of NF-κB may cause abnormal release of inflammatory mediators, promote chronic inflammation, and disrupt immune homeostasis. Therefore, precise regulation of NF-κB activation is important for maintaining immune balance (Chen et al. 2023). In recent years, natural polysaccharides have been reported to regulate macrophage immune functions through the NF-κB signaling pathway. Some plant- and algae-derived polysaccharides can promote NF-κB p65 nuclear translocation and increase the expression of immune-related factors such as iNOS, TNF-α, and IL-6, thereby promoting macrophage activation and enhancing immune responses (Xie et al. 2019; Yang et al. 2019; Tabarsa et al. 2020).

Based on this background, the present study used RAW264.7 macrophages as an in vitro model to evaluate the immunostimulatory activity of PSP and investigate its effects on macrophage immune functions. We further examined whether PSP promotes the expression of immune-related factors through regulation of the NF-κB signaling pathway. The results may provide a theoretical basis for understanding the immunomodulatory mechanism of PSP and support further investigation of PSP as a natural immunomodulatory bioactive component.

2 Materials and methods

2.1 Materials and reagents

The fresh *Spirulina platensis* was provided by Gansu Kaiyuan Biotech-nology Development Center Co., Ltd. (Gansu, China).

2.2 Extraction, isolation, and purification of polysaccharides

Crude polysaccharides were extracted using a water extraction method (solid-to-liquid ratio of 1:40) combined with an alcohol precipitation method (95% ethanol) at 70 °C for 120 min. Protein was removed from the crude polysaccharides using the Sevag method (chloroform:n-butanol volume ratio of 4:1), and the solution was scanned over the wavelength range of 190–400 nm using a UV-Vis spectrophotometer to determine the presence of proteins and nucleic acids. In the absence of absorption peaks for proteins and nucleic acids, the organic solvent in the solution was removed using a rotary evaporator. The collected solution was dialyzed and then freeze-dried to obtain the deproteinized polysaccharide, designated C-PSP.

After the chromatography column was thoroughly cleaned, fixed, and wetted, Sephadex G-200 medium was slowly poured along the inner wall. Following uniform packing and natural sedimentation, the column was equilibrated with distilled water overnight. Subsequently, 0.5 mL of membrane-filtered C-PSP-1 solution was loaded onto the column and eluted at a flow rate of 0.2 mL min^{-1}. Fractions of 2 mL per tube were collected, and the absorbance at 490 nm was determined by the phenol-sulfuric acid method to plot the elution curve. The sugar solution corresponding to the peak apex was collected and freeze-dried to obtain Polysaccharides from *Spirulina platensis* (PSP).

2.3 Sugar and uronic acid contents

The total sugar content was determined using the phenol-sulfuric acid method. A *Spirulina platensis* polysaccharide solution at a concentration of 1 mg mL^{-1} was prepared. Following a ratio of 1:1:5, 1 mL of the polysaccharide solution, 1 mL of 5% phenol solution, and 5 mL of concentrated sulfuric acid were mixed and allowed to stand for 30 min. The absorbance was measured at 490 nm, and the total sugar content of the sample was calculated based on the standard curve.

The uronic acid content was determined using the sulfuric acid–carbazole method. Aliquots of 0.00, 0.10, 0.20, 0.30, 0.40, 0.50, and 0.60 mL of a 1.00 mg mL^{-1} galacturonic acid standard solution were each transferred to 10 mL volumetric flasks and brought to volume with water. From each standard solution, 1.00 mL was transferred into a 20 mL stoppered colorimetric tube.

Under ice-bath conditions, 5.0 mL of sulfuric acid solution was added. After vortex mixing, the mixture was heated in a boiling water bath for 5 min, cooled in an ice bath, and then 100 μL of 1.5 mg mL^{-1} m-hydroxybiphenyl solution was added, followed by shaking for 5 min and ultrasonic defoaming. A control group was prepared in the same manner using 1.0 mL of water. The absorbance was measured at 524 nm. A standard curve was plotted with uronic acid mass concentration as the abscissa and absorbance as the ordinate, and the uronic acid content in PSP was calculated accordingly.

2.4 Physicochemical Analysis of PSP

2.4.1 Molecular Weight Determination

Dextran standards (T-10, T-40, T-70, T-110, T-500, T-2000) and PSP, each precisely weighed at 2.0 mg, were dissolved in 1.0 mL of ultrapure water and filtered through a 0.22 μm aqueous membrane prior to HPLC analysis. The chromatographic conditions were as follows: column, TSK gel G4000P WXL-CP (7.8 mm × 300 mm); sample and standard concentrations, 2 mg mL^{-1}; injection volume, 20 μL; column temperature, 30 °C; refractive index detector temperature, 35 °C; mobile phase, ultrapure water at a flow rate of 0.6 mL min^{-1}. The retention times of each dextran standard and PSP were recorded. A standard curve was established by plotting the logarithm of the molecular weight of the standards (ordinate) against their retention times (abscissa), and the molecular weight of PSP was calculated based on its retention time.

2.4.2 FT-IR Analysis

PSP (2 mg) was mixed thoroughly with KBr, ground in a mortar, and pressed into a transparent pellet. The FT-IR spectrum was recorded over the scanning range of 500–4000 cm^{-1}.

2.4.3 Monosaccharide Composition Analysis

PSP and the monosaccharide standards (mannose, rhamnose, glucose, galactose, xylose, and arabinose), each precisely weighed at 5 mg, were placed in 10 mL ampoule bottles. Trifluoroacetic acid (3 mL, 2 mol L^{-1}) was added, and the ampoules were sealed with an alcohol blast burner and hydrolyzed in an oil bath at 110 °C for 4 h. The hydrolysates were concentrated by rotary evaporation at 60 °C until no organic solvent odor remained, and then redissolved in

4 mL of ultrapure water. A 400 μL aliquot of the sample solution was transferred to a 5 mL centrifuge tube, and equal volumes of 0.5 mol L^{-1} PMP methanol solution and 0.3 mol L^{-1} NaOH solution were added sequentially. The tube was sealed with plastic wrap and derivatized in a water bath at 70 °C for 100 min. After the reaction, 500 μL of 0.3 mol L^{-1} HCl was added for neutralization, followed by extraction with chloroform four times. The aqueous phase was collected and filtered through a 0.22 μm aqueous membrane. The chromatographic conditions were as follows: mobile phase A, acetonitrile; mobile phase B, 0.05 mol L^{-1} KH_2PO_4 solution (pH 6.80); flow rate, 1.0 mL min^{-1}; injection volume, 10 μL; column temperature, 25 °C; detection wavelength, 254 nm. The gradient elution program was: 0–5 min, 17%-18% A; 5–10 min, 18%-19% A; 10–30 min, 19%-20% A; 30–50 min, 17% A.

2.4.4 Congo Red Assay

PSP solution (2 mL, 1 mg mL^{-1}) was added to a test tube and mixed by vortexing. Sodium hydroxide solution (1 mol L^{-1}) was added to achieve final NaOH concentrations of 0, 0.1, 0.2, 0.3, 0.4, and 0.5 mol L^{-1}. The mixtures were allowed to stand at room temperature for 5 min, and the maximum absorption wavelength was scanned using a UV-Vis spectrophotometer over the range of 400–600 nm (Zhang et al. 2021).

2.4.5 TG Analysis

Thermogravimetric analysis was performed using a thermogravimetric analyzer. PSP (5 mg) was weighed and analyzed under a nitrogen atmosphere at a flow rate of 60 mL min^{-1}. The initial temperature was set at 30 °C, and the sample was heated to a final temperature of 600 °C at a heating rate of 10 °C min^{-1} with a scanning rate of 1 °C min^{-1} (Kumar and Jayaram 2017).

2.4.6 SEM Analysis

PSP (2 mg) was mounted onto double-sided adhesive tape and sputter-coated with gold. The surface morphology of the sample was observed using a scanning electron microscope at magnifications of 500× and 1000×, and images were captured after adjusting to a clear field of view.

2.5 Immunomodulatory activity

2.5.1 Cell viability

RAW264.7 macrophages in the logarithmic growth phase were harvested, adjusted to 1.0×10^5 cells mL^{-1}, and seeded into 96-well plates at 100 μL per well. After cell adhesion, the cells were treated with PSP at final concentrations of 25, 50, 100, 200, or 400 μg mL^{-1}. LPS (1 μg mL^{-1}) was used as the positive control, and untreated cells served as the control group. The cells were incubated in complete medium containing 15% fetal bovine serum and 1% penicillin-streptomycin at 37 °C with 5% CO_2 for 24 h. CCK-8 reagent (10 μL) was then added to each well, followed by incubation for 1 h at 37 °C. Absorbance was measured at 450 nm, and cell viability was calculated relative to the control group.

2.5.2 Neutral red phagocytosis

RAW264.7 macrophages in the logarithmic growth phase were adjusted to 1.0×10^5 cells mL^{-1} and seeded into 96-well plates at 100 μL per well. After cell adhesion, the cells were treated with PSP at final concentrations of 50, 100, or 200 μg mL^{-1}. LPS (1 μg mL^{-1}) was used as the positive control, and untreated cells served as the control group. After incubation for 24 h at 37 °C, the medium was removed and 100 μL of 0.1% neutral red solution was added to each well. The cells were incubated for 1 h, washed three times with PBS, and lysed with 100 μL of cell lysis buffer. After shaking in the dark for 30 min, absorbance was measured at 540 nm and the phagocytic rate was calculated. Six replicate wells were used for each group, and the experiment was independently repeated three times.

2.5.3 Nitric oxide secretion

RAW264.7 macrophages in the logarithmic growth phase were adjusted to 2×10^5 cells mL^{-1}, seeded into 24-well plates at 1 mL per well, and cultured for 12-16 h. The medium was then removed. The experimental groups received 2 mL of PSP at final concentrations of 50, 100, or 200 μg mL^{-1}, the positive-control group received 2 mL of LPS (1 μg mL^{-1}), and the blank-control group received 2 mL of complete medium. Three replicate wells were used for each group. After incubation for 24 h, the culture supernatants were collected and centrifuged.

Supernatant (50 μL) was mixed sequentially with 50 μL each of Griess reagents A and B in a 96-well plate and incubated in the dark for 15 min. Absorbance was measured at 540 nm, and NO concentration was determined from the standard curve.

2.5.4 Effects of PSP on the Gene Expression of Immune Regulatory Factors by RAW264.7 Macrophages

RAW264.7 macrophages were adjusted to 1×10^6 cells mL^{-1}, seeded into 6-well plates, and cultured for 24 h at 37 °C with 5% CO_2. The cells were then divided into an untreated control group, an LPS group (1 μg mL^{-1}), and a PSP group (50 μg mL^{-1}) and incubated for a further 24 h. Total RNA was collected at the end of treatment for quantitative real-time PCR analysis of IL-6, TNF-α, COX-2, and iNOS expression.

RNA extraction. Total RNA was extracted from RAW264.7 macrophages using an RNA extraction kit according to the manufacturer's instructions. RNA that met the quality requirements was used for complementary DNA synthesis.

Reverse transcription. The reverse-transcription mixture contained 2 μL of total RNA, 3 μL of 5× gDNA digester Mix, and 10 μL of Nuclease-Free Water. The reaction was performed at 25 °C for 5 min, 55 °C for 15 min, and 85 °C for 5 min. The resulting complementary DNA was diluted tenfold before quantitative PCR.

Quantitative PCR. Quantitative PCR was performed in 0.1-mL reaction plates using the reaction mixture shown in Table. 1 and the primers listed in Table. 2 The program consisted of pre-denaturation at 95 °C for 10 min, followed by 40 cycles of denaturation at 95 °C for 10 s and annealing and extension at 57 °C for 20 s. Melt-curve analysis was then performed from 72 to 95 °C with fluorescence recorded at 0.5 °C intervals.

Relative-expression analysis. Relative gene expression was calculated using the $2^{-\Delta\Delta Ct}$ method, where $\Delta Ct = Ct(target\ gene) - Ct(reference\ gene)$ and $\Delta\Delta Ct = \Delta Ct(sample) - \Delta Ct(control)$.

Component	Volume (μL)
2×Universal Blue SYBR Green qPCR Master Mix	10 μL
Forward primer	1 μL

Reverse primer	1 μL
reverse transcription product	2 μL
Nuclease-free water	6 μL

Table. 1 Quantitative PCR reaction mixture

Primer	Primer sequence (5′–3′)
β-actin	Forward: 5′–TGCTGTCCCTGTATGCCTCT–3′ Reverse: 5′–TTTGATGTCACGCACGATTT–3′
TNF-α	Forward: 5′–CCCTCCTGGCCAACGGCATG–3′ Reverse: 5′–TCGGGGCAGCCTTGTCCCTT–3′
IL-6	Forward: 5′–AGACAAAGCCAGAGTCCTTCAGAGA–3′ Reverse: 5′–GCCACTCCTTCTGTGACTCCAGC–3′
iNOS	Forward: 5′–GCTCGCTTTGCCACGGACGA–3′ Reverse: 5′–AAGGCAGCGGGCACATGCAA–3′
COX-2	Forward: 5′–GGGCTCAGCCAGGCAGCAAAT–3′ Reverse: 5′–GCACTGTGTTTGGGGTGGGCT–3′

Table. 2 Primer sequences used for quantitative PCR

2.5.5 Effect of PSP on the Secretion of Cytokines by RAW264.7 Macrophages

RAW264.7 macrophages in the logarithmic growth phase were seeded into 6-well plates at 2×10^6 cells $well^{-1}$. After cell adhesion, the cells were assigned to the untreated control, LPS, and PSP groups using the treatments described in Section 2.5.4 and incubated for 24 h. The culture supernatants were collected, and IL-6 and TNF-α concentrations were determined using the corresponding ELISA kits and calculated from their standard curves.

2.5.6 Western Blot Analysis of Cytokine Expression

RAW264.7 macrophages were adjusted to 5×10^6 cells mL^{-1}, seeded into 6-well plates, and cultured for 24 h at 37 °C with 5% CO_2. The cells were then assigned to an untreated control group, an LPS group (5 μg mL^{-1}), and a PSP group (50 μg mL^{-1}) and incubated for a further 24 h. Three replicate wells were used for each group. After treatment, the cells were washed twice with PBS and lysed with RIPA buffer on ice. Total protein was extracted under low-temperature conditions, heat-denatured, and stored for Western blot analysis.

SDS-PAGE. Protein samples (20 μg per lane) were separated using stacking and resolving gels. Electrophoresis was performed at 80 V for 30 min and then at 120 V for 120 min.

Membrane transfer. The separated proteins were transferred to a PVDF membrane at a constant current of 400 mA for 90 min in an ice-water bath.

Immunodetection. The PVDF membrane was washed with TBST and blocked with non-fat milk for 2 h. The membrane was incubated with primary antibodies for 16 h and secondary antibodies for 2 h and washed four times with TBST. Protein bands were visualized using ECL reagent and recorded with an ImageQuant LAS 4000 mini chemiluminescence imaging system. The relative phosphorylation levels of IκBα and p65 were evaluated from the p-IκBα/IκBα and p-p65/p65 ratios.

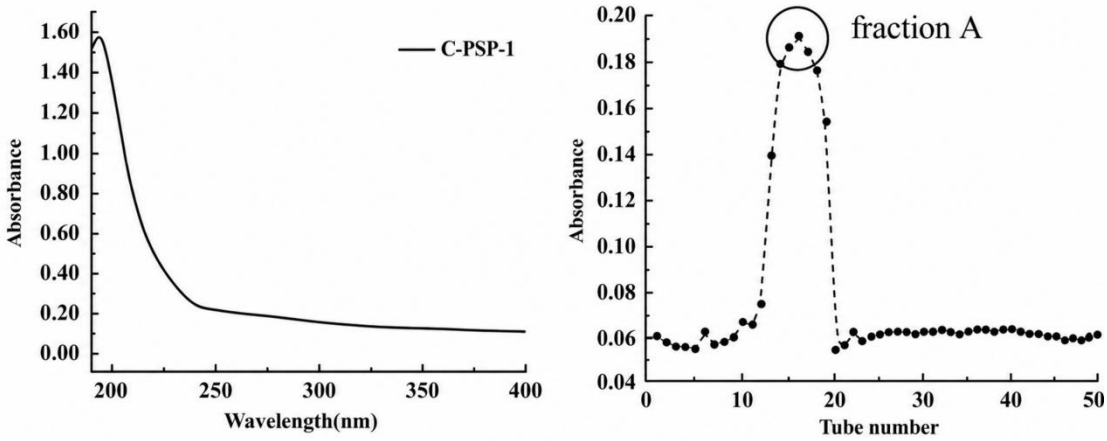
2.6 Statistical analysis

All experiments were performed in triplicate, and the arithmetic mean of the three parallel experiments was taken as the result. Correlation analysis was performed using SPSS software. A value of $p < 0.05$ was considered statistically significant.

3 Results

3.1 Preparation of PSP

As shown in Fig. 1(a), the full-wavelength scanning spectrum of C-PSP shows no absorption peaks at 260-280 nm, indicating the absence of proteins, peptides, and nucleic acids in C-PSP. C-PSP was separated and purified by Sephadex G-200 gel column chromatography, and the elution curve is presented in Fig. 1(b). Fraction A was collected, freeze-dried, and designated as PSP.



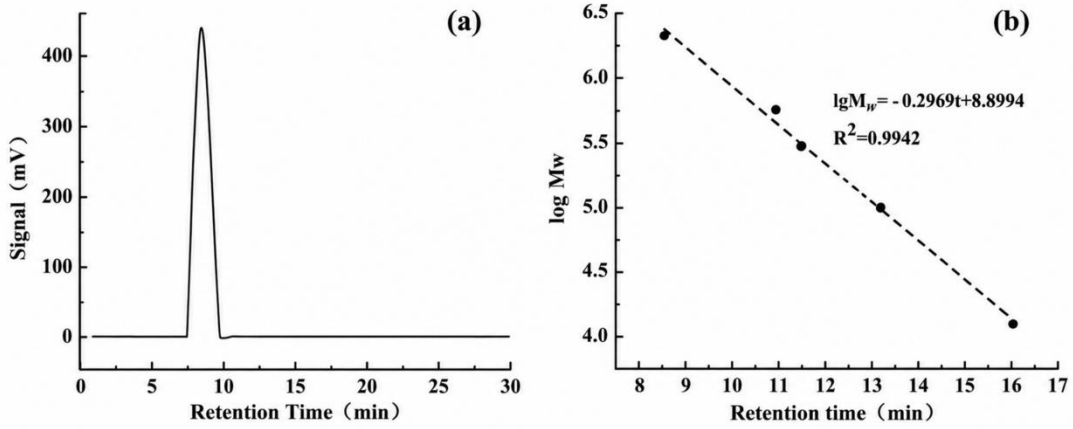
(a) Full-wavelength scanning spectrum (b) Elution profile

Fig. 1 Preparation of PSP

3.2 Physicochemical characterization

3.2.1 Molecular Weight Determination

As shown in the liquid chromatogram in Fig. 2(a), the peak of PSP appeared at 8.401 min as a single, symmetrical peak. The total sugar content of PSP was determined to be 91.03 ± 0.35% by the phenol-sulfuric acid method, and no uronic acid was detected by the sulfuric acid-carbazole method. Taken together, these results indicate that PSP is a neutral polysaccharide with uniform molecular weight distribution and high purity. Based on the dextran standards presented in Fig. 2(b), the molecular weight of PSP was calculated to be 2.54×10^{6} Da.



(a) HPLC chromatogram of PSP (b) Standard Curve of Molecular Weight Standards.

Fig. 2 Purity and molecular-weight determination

3.2.2 FT-IR Analysis

The absorption peak at 3290.23 cm^{-1} is attributed to the stretching vibration of hydroxyl groups (-OH); the absorption at 2928.62 cm^{-1} corresponds to the C-H stretching vibration of methyl and methylene groups; the absorption peaks at 1644.94 cm^{-1} and 1411.68 cm^{-1} are assigned to the H-O-H bending vibration of water and the C-H bending vibration on the sugar ring, respectively; the peak at 1230.86 cm^{-1} is due to the bending vibration of hydroxyl groups (-OH); and the absorption near 1046.08 cm^{-1} is caused by C-O bending vibration, indicating the presence of a pyranose ring structure in the molecule. No characteristic absorption peak of carboxyl groups (-COOH) was observed in the spectrum, suggesting the absence of uronic acid in PSP (Fig. 3).

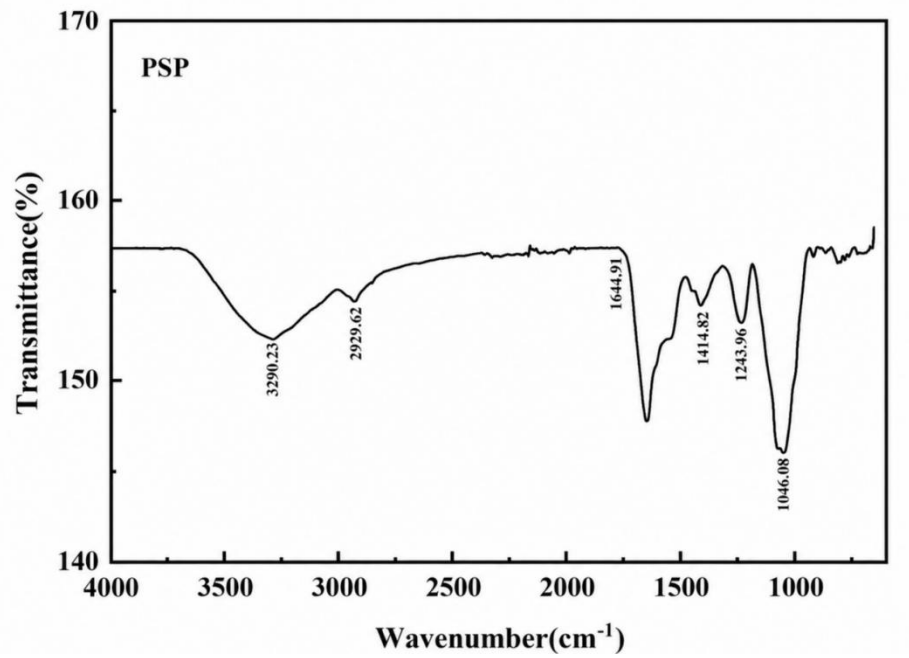
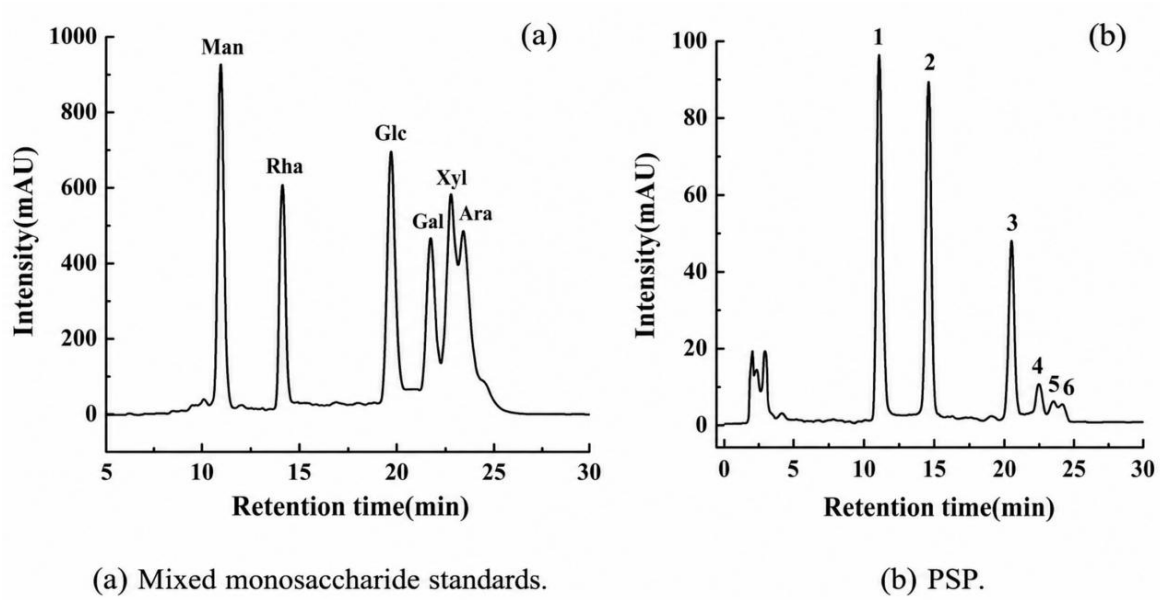


Fig. 3 FT-IR spectrum of PSP

3.2.3 Monosaccharide composition analysis

The monosaccharide composition of PSP was analyzed by HPLC. The molar ratio of monosaccharides in PSP was mannose : rhamnose : glucose : galactose : xylose : arabinose = 36.32 : 33.24: 20.83 : 4.52 : 2.84 : 2.26, confirming that PSP is a neutral heteropolysaccharide predominantly composed of mannose (Fig. 4).



(a) Mixed monosaccharide standards. (b) PSP.

Fig. 4 Monosaccharide composition of PSP

3.2.5 Congo Red Assay

After mixing PSP with Congo red, the maximum absorption wavelength shifted from 496-504 nm, moving toward longer wavelengths, indicating a clear red shift (Fig. 5). This suggests that PSP possesses a triple-helix structure. The triple-helix structure is a highly ordered spatial conformation that confers high thermal and chemical stability to PSP [34].

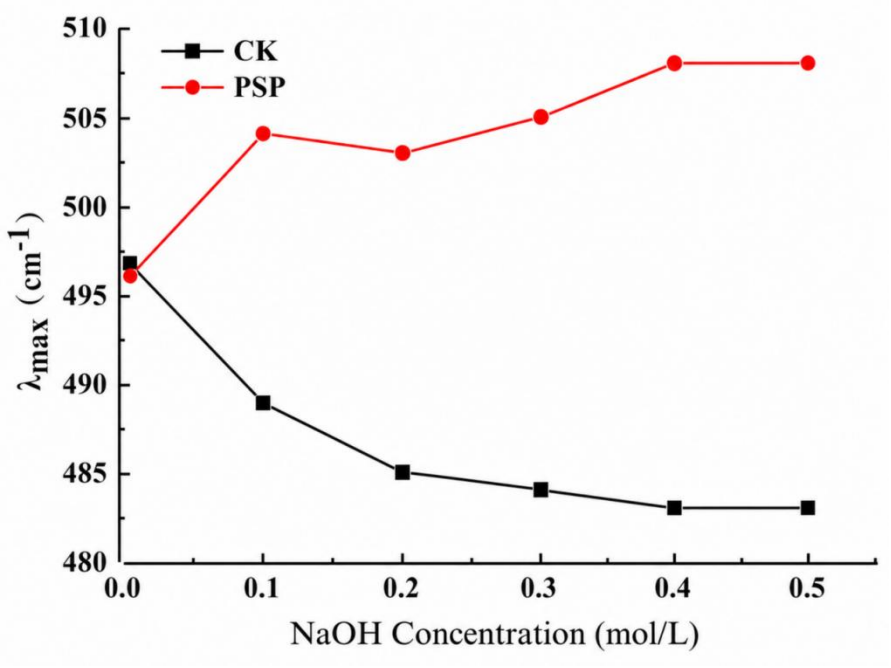


Fig. 5 Congo red assay of PSP

3.2.5 TG Analysis

The thermal stability of PSP was shown in Fig. 6.In the first stage, within the temperature range of 40-230°C, the mass loss of PSP was primarily attributed to free water and bound water, resulting in an 8.366% decrease in mass. The second stage, occurring between 230°C and 450°C, shows a significant loss of polysaccharide mass, reaching 61.221%. The third stage, as the temperature rises from 500°C to 600°C, involves the breaking of chemical bonds and the decomposition of the substance; the thermal degradation process of the polysaccharide is essentially complete, and the loss stabilizes. In summary, PSP exhibits good thermal stability below 230°C but begins to decompose above 230°C.

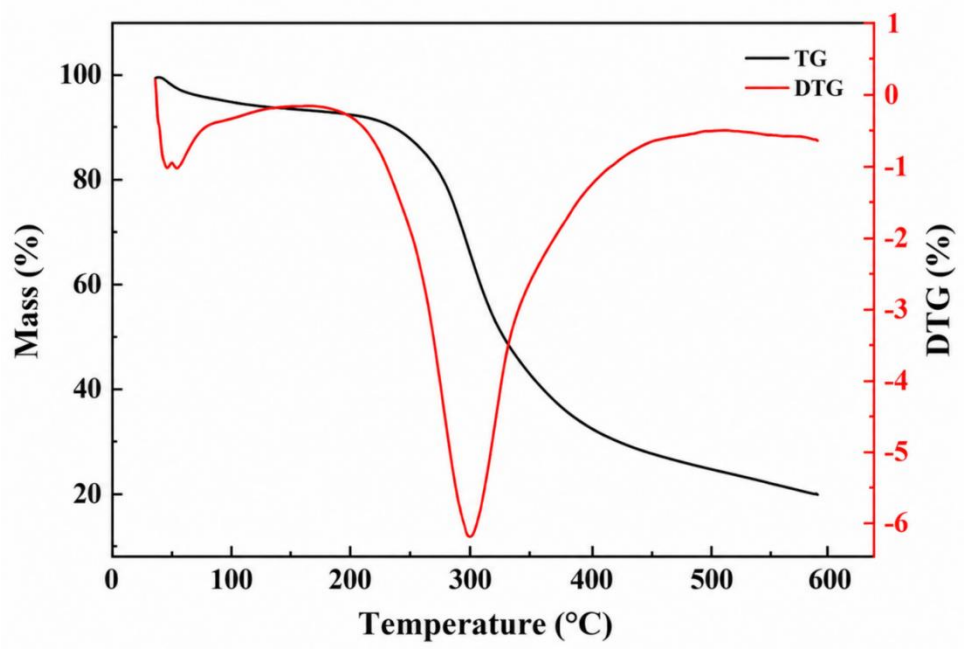
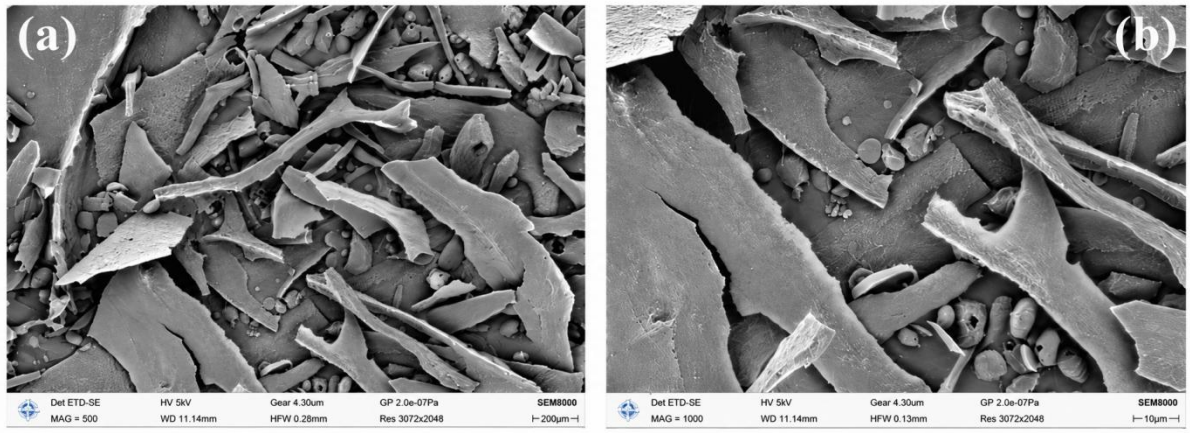


Fig. 6 Thermogravimetric analysis of PSP

3.2.6 SEM Analysis

PSP was observed by SEM(Fig. 7), As shown in the 500× magnified image , PSP exhibits a mixed morphology of irregularly stacked flakes and rods; The image at 1000× magnification further shows that the edges of PSP fragments are irregularly torn, while the surface is relatively smooth with only a small number of pits and protrusions. This layered stacking structure indicates that intermolecular interactions primarily occur via hydrogen bonds and van der

Waals forces, rather than through a crystalline structure. This is consistent with the abundant hydroxyl (-OH) vibrations observed in the FT-IR spectrum.



(a) PSP SEM image at 500×magnification (b) PSP SEM image at 1000×magnification

Fig. 7 SEM images of native polysaccharide PSP

3.3 Immunomodulatory activity

3.3.1 Cell viability

PSP at 25-200 μg mL^{-1} produced RAW264.7 cell-viability values above the untreated control ($p < 0.05$), with the largest responses at 25 and 50 μg mL^{-1} (Fig. 8). The response declined as the concentration increased, and viability at 400 μg mL^{-1} was below the untreated control ($p < 0.05$).

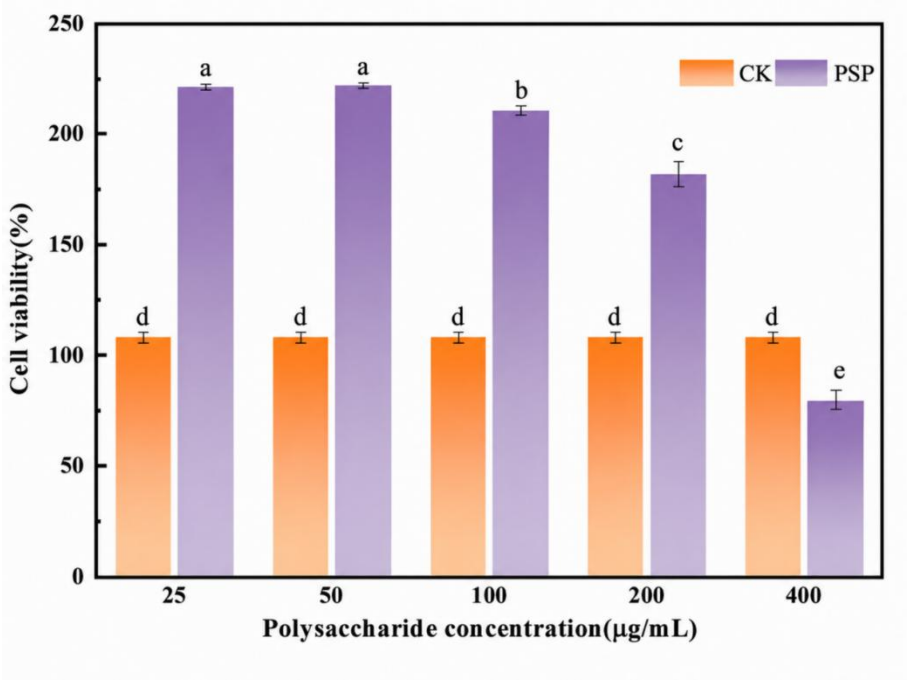
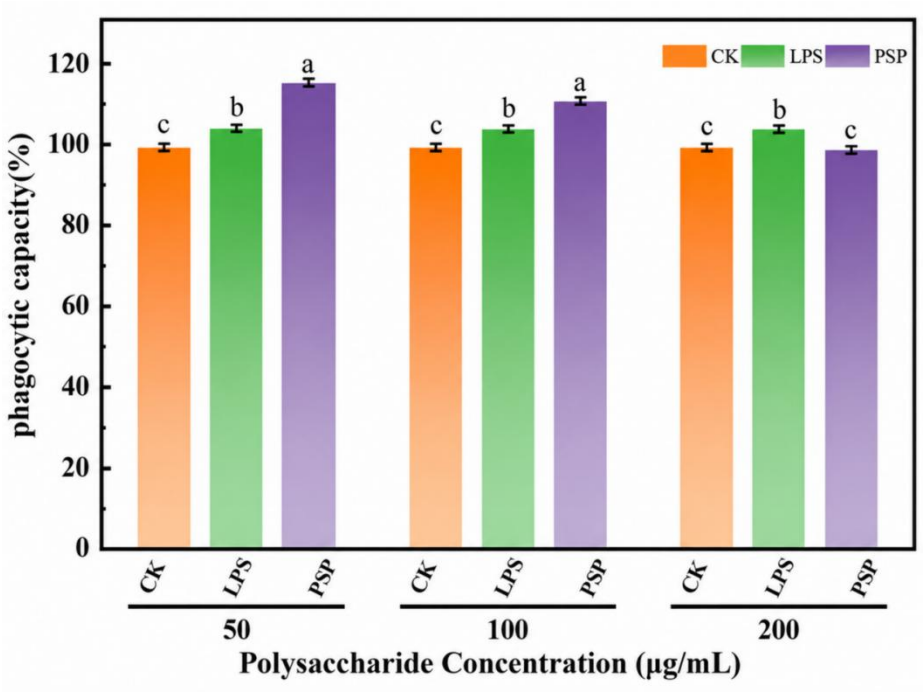


Fig. 8 Effects of PSP concentration on RAW264.7 cell viability

3.3.2 Neutral red phagocytosis

As shown in Fig. 9, PSP at a concentration of 50 μg mL^{-1} significantly enhanced the phagocytic capacity of the cells, with the effect being superior to both the control group group and the LPS group ($p < 0.05$). At 100 μg mL^{-1}, PSP still exhibited a significant promoting effect, although the intensity of the effect was somewhat reduced. At 200 μg mL^{-1}, the phagocytic capacity was lower than that of the LPS group and showed no significant difference compared with the control group group ($p > 0.05$).

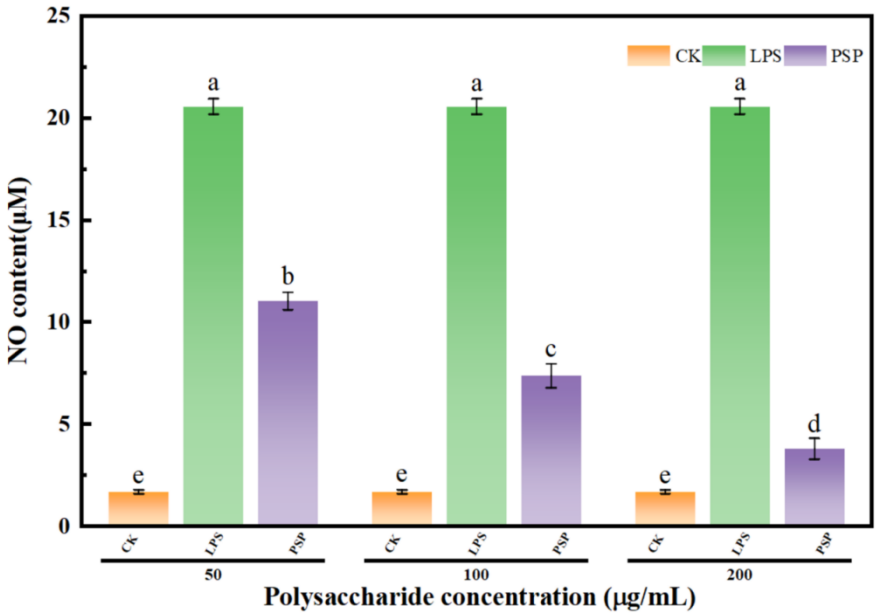


365

366 Fig. 9 Effects of PSP concentration on neutral red uptake by RAW264.7 macrophages

367 **3.3.3 Nitric oxide secretion**

368 As shown in Fig. 10, compared with the control group group, PSP at all tested
369 concentrations significantly promoted NO release ($p<0.05$). Among them, 50 μg mL^{-1} PSP
370 exhibited the optimal effect, although its secretory promoting capacity was still weaker than
371 that of the LPS group. The inductive effect decreased at 100 μg mL^{-1} PSP and was further
372 diminished at 200 μg mL^{-1}, with only a weak activation effect remaining.



373

374 Fig. 10 Effects of PSP concentration on nitric oxide release by RAW264.7 cells

375 **3.3.4 Effects of PSP on the Gene Expression of Immune Regulatory Factors by RAW264.7**

376 **Macrophages**

377 The mRNA expression levels of core inflammatory enzymes (COX-2, iNOS) and pro-

378 inflammatory cytokines (IL-6, TNF-α) following PSP treatment are shown in Fig. 11.

379 Compared with the control group group, the expression of the above genes was significantly

380 upregulated in PSP-treated group ($p<0.05$).

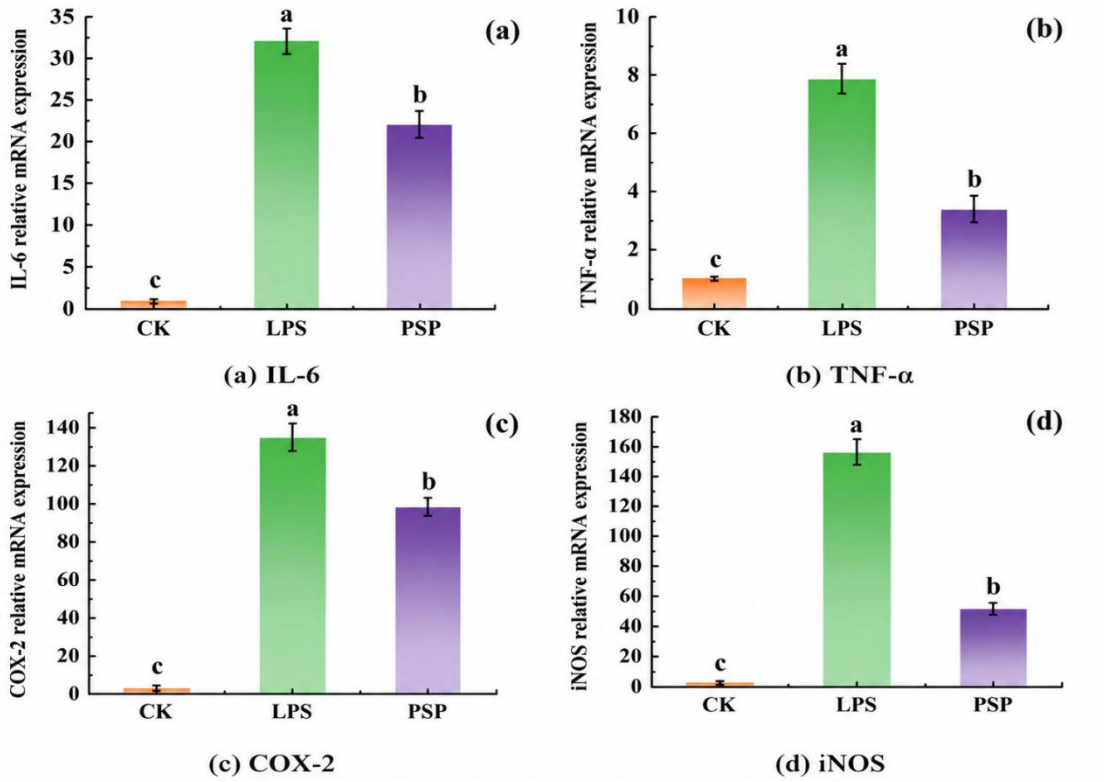
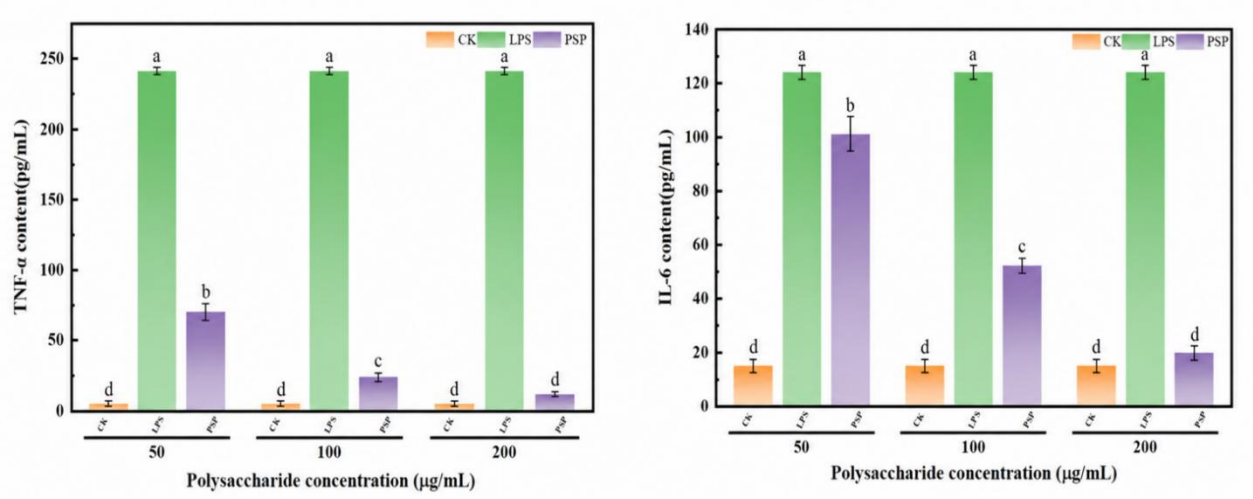


Fig. 11 Effects of PSP on IL-6, TNF-α, COX-2, and iNOS expression in RAW264.7 cells

3.3.5 Effect of PSP on the Secretion of Cytokines by RAW264.7 Macrophages

As shown in Fig. 12, compared with the control group , the PSP-treated groups significantly induced the secretion of the cytokines IL-6 and TNF-α in RAW264.7 macrophages ($p<0.05$). Furthermore, the increased secretion of the cytokines IL-6 and TNF-α following PSP treatment is consistent with the upregulation of IL-6 and TNF-α gene expression observed in Section 2.3.4.



(a) TNF-α (b) IL-6

Fig. 12 Effects of PSP concentration on cytokine secretion by RAW264.7 cells

3.3.6 Western Blot Analysis of Cytokine Expression

As shown in Fig. 13, after PSP treatment, the p-IκBα and p-P65 bands were more distinct than those in the control group, indicating that the polysaccharide activated the phosphorylation of IκBα and also increased the phosphorylation level of p65. Data analysis revealed that, compared with the control group group, the p-IκBα/IκBα and p-P65/P65 ratios in cells were both elevated after PSP treatment ($p<0.05$), indicating that PSP promotes the phosphorylation of IκBα and p65.

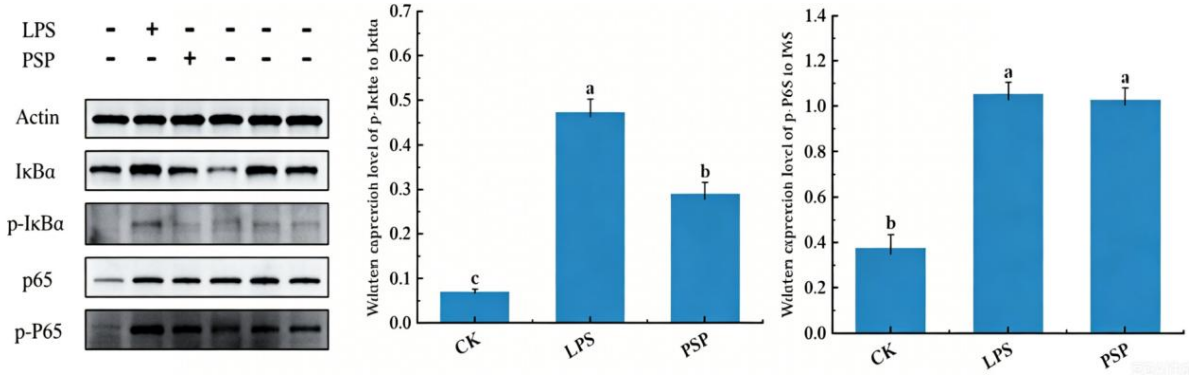


Fig. 13 Effects of PSP on NF-κB pathway proteins in RAW264.7 cells

4 Discussion

The absence of absorption peaks at 260-280 nm, together with the single symmetrical

chromatographic peak, indicates that PSP was effectively purified and had a uniform molecular weight distribution. PSP was composed mainly of mannose, rhamnose, and glucose and contained no detectable uronic acid, confirming that it is a mannose-rich neutral heteropolysaccharide. The compositional diversity of polysaccharides from Arthrospira is affected by the source material and by extraction and purification procedures (Cai et al. 2022; Ai et al. 2023; Fan et al. 2026). In the present study, the shift in the maximum absorption wavelength after interaction with Congo red supports the presence of an ordered triple-helical conformation (Zhang et al. 2021). The abundant hydroxyl groups detected by FT-IR, the irregular sheet-like morphology, and the thermal stability below 230 °C further define the physicochemical characteristics of PSP (Kumar Varma and Jayaram Kumar 2017). These results establish the structural basis for its macrophage-modulating activity, thereby providing a basis for elucidating the mechanism of action of this activity.

PSP significantly enhanced RAW264.7 cell viability, neutral red uptake, and NO release, demonstrating activation of macrophage functions at the cellular level. The strongest responses occurred mainly at 25 or 50 μg mL^{-1} and declined as the concentration increased, showing that the activity of PSP depends on an appropriate concentration range. Similar concentration-dependent responses have been observed for other natural polysaccharides (Wang et al. 2024b; Jin et al. 2025). Enhanced neutral red uptake represents increased macrophage phagocytic capacity (Brown 2024), consistent with the effects reported for polysaccharides from Pueraria lobata, Polygonatum sibiricum, Sinonovacula constricta, and Cucurbita moschata (Liu et al. 2018; Dong et al. 2020; Huang et al. 2021; Liu et al. 2022;). NO is an important effector molecule produced by activated macrophages and participates in immune defense and intercellular signaling (Bogdan 2015; Lundberg and Weitzberg 2022; Wu et al. 2023; Xiang et al. 2024). The response observed here is also consistent with the macrophage-activating activity previously reported for Arthrospira polysaccharides (Wu et al. 2020). Thus, the increases in cell viability, phagocytic activity, and NO release provide mutually supporting functional evidence that PSP activates RAW264.7 macrophages.

The functional activation of macrophages was accompanied by coordinated molecular responses. PSP increased the messenger RNA abundance of IL-6, TNF-α, COX-2, and iNOS

and simultaneously promoted the secretion of IL-6 and TNF-α. The agreement between transcriptional induction and cytokine secretion demonstrates that the effect of PSP was transmitted from gene regulation to the production of immune mediators. IL-6 and TNF-α coordinate macrophage-dependent immune responses (Eddahri et al. 2009; Popko et al. 2010; Kwon et al. 2020), while COX-2-derived prostaglandins and iNOS-derived NO are important components of inflammatory and immune regulation (Ricciotti and FitzGerald 2011; Song et al. 2021; Wang et al. 2026). Therefore, the increased expression of these genes explains, at least in part, the enhanced NO release and cytokine production and links the observed cellular responses to a defined transcriptional program.

NF-κB provides the mechanistic connection between these molecular and functional responses. In resting macrophages, NF-κB is retained in the cytoplasm by IκBα. Phosphorylation of IκBα promotes release of the NF-κB complex, whereas phosphorylation of p65 enhances its transcriptional activity and drives the expression of immune-related genes, including those examined in this study (Oeckinghaus et al. 2011; Liu et al. 2017; Xu et al. 2021; Guo et al. 2024; Hoffmann et al. 2025; Mao et al. 2025). PSP significantly increased both the p-IκBα/IκBα and p-p65/p65 ratios. These protein-level changes, together with the coordinated increases in IL-6, TNF-α, COX-2, and iNOS expression, demonstrate that activation of the classical NF-κB pathway is a central mechanism underlying the immunomodulatory activity of PSP. This interpretation is supported by related studies in which natural polysaccharides activated macrophage functions through NF-κB-associated signaling (Li et al. 2022; Zheng and Huang 2022; Li et al. 2023a; Li et al. 2024; Wang et al. 2024a; Li et al. 2025).

The structural features of PSP may contribute to the initiation of this signaling chain. Its high mannose proportion indicates mannose-rich structural domains, which have been associated with macrophage recognition and downstream signaling in related polysaccharides (Li et al. 2022; Niu et al. 2023; Shang et al. 2026). Its triple-helical conformation also provides an ordered spatial structure that may facilitate the interaction of polysaccharides with immune-cell receptors (Satitmanwiwat et al. 2012; Zheng and Huang 2022; Kumar et al. 2023). Accordingly, the mannose-rich composition and ordered conformation of PSP provide a plausible structural basis for the NF-κB activation and immunomodulatory responses observed

in this study. However, the receptor responsible for PSP recognition was not directly examined, and the current experiments do not establish a direct structure–receptor interaction. Because the biological evaluation was performed in an in vitro RAW264.7 macrophage model, receptor-intervention experiments and in vivo studies are required to further define the upstream recognition mechanism, dose-response relationship, and biological safety of PSP.

5 Conclusions

PSP is a neutral heteropolysaccharide extracted from *Spirulina platensis* and is composed of mannose, rhamnose, glucose, galactose, xylose, and arabinose at a molar ratio of 36.32:33.24:20.83:4.52:2.84:2.26. Within the tested non-cytotoxic concentration range, PSP activated NF-κB signaling, enhanced immune regulation at the transcriptional level, increased RAW264.7 macrophage viability and phagocytic capacity, and promoted the production of NO, IL-6, and TNF-α. These results demonstrate the in vitro immunomodulatory activity of PSP and establish it as a bioactive component worthy of further investigation for immunomodulatory applications.

References

Ai X, Yu P, Li X, Lai X, Yang M, Liu F, Luan F, Meng X (2023) Polysaccharides from Spirulina platensis: Extraction methods, structural features and bioactivities diversity. Int J Biol Macromol 231:123211.

Barnabei L, Laplantine E, Mbongo W, Rieux-Laucat F, Weil R (2021) NF-κB: At the borders of autoimmunity and inflammation. Front Immunol 12:716469.

Bogdan C (2015) Nitric oxide synthase in innate and adaptive immunity: An update. Trends Immunol 36:161-178.

Brown GC (2024) Cell death by phagocytosis. Nat Rev Immunol 24:91-102.

Cai B, Zhao X, Luo L, Wan P, Chen H, Pan J (2022) Structural characterization, and in vitro immunostimulatory and antitumor activity of an acid polysaccharide from Spirulina platensis. Int J Biol Macromol 196:46-53.

Chen S, Saeed AFUH, Liu Q, Jiang Q, Xu H, Xiao GG, Rao L, Duo Y (2023) Macrophages in immunoregulation and therapeutics. Signal Transduct Target Ther 8:207.

Christofides A, Strauss L, Yeo A, Cao C, Charest A, Boussiotis VA (2022) The complex role of tumor-infiltrating macrophages. Nat Immunol 23:1148-1156.

Dong Z, Zhang M, Li H, Zhan Q, Lai F, Wu H (2020) Structural characterization and immunomodulatory activity of a novel polysaccharide from Pueraria lobata (Willd.) Ohwi root. Int J Biol Macromol 154:1556-1564.

Dorrington MG, Fraser IDC (2019) NF-κB signaling in macrophages: Dynamics, crosstalk, and signal integration. Front Immunol 10:705.

Eddahri F, Denanglaire S, Bureau F, Spolski R, Leonard WJ, Leo O, Andris F (2009) Interleukin-6/STAT3 signaling regulates the ability of naive T cells to acquire B-cell help capacities. Blood 113:2426-2433.

Fan B, Jiang M, Mi Y, Yuan X, Li M (2026) Extraction, analysis, and identification methods of active components from Rhizoma polygonati, Polygonatum notoginseng, and Portulaca oleracea. In: Kong Z, Li M, Wang Y, Zhang Z (eds) Smart and Green Production

513 Technologies for Traditional Chinese Medicinal Materials. Springer, Singapore, pp 51-99.

514 Franken L, Schiwon M, Kurts C (2016) Macrophages: Sentinels and regulators of the immune
515 system. Cell Microbiol 18:475-487.

516 Fratelli C, Bürck M, Amarante MCA, Braga ARC (2021) Antioxidant potential of nature's
517 "something blue": Something new in the marriage of biological activity and extraction
518 methods applied to C-phycocyanin. Trends Food Sci Technol 107:309-323.

519 Fu Y, Jiao H, Sun J, Okoye CO, Zhang H, Li Y, Lu X, Wang Q, Liu J (2024) Structure-activity
520 relationships of bioactive polysaccharides extracted from macroalgae towards biomedical
521 application: A review. Carbohydr Polym 324:121533.

522 Guo Q, Jin Y, Chen X, Ye X, Shen X, Lin M, Zeng C, Zhou T, Zhang J (2024) NF-κB in biology
523 and targeted therapy: New insights and translational implications. Signal Transduct Target
524 Ther 9:53.

525 Hamedifard Z, Milajerdi A, Reiner Ž, Taghizadeh M, Kolahdooz F, Asemi Z (2019) The effects
526 of spirulina on glycemic control and serum lipoproteins in patients with metabolic
527 syndrome and related disorders: A systematic review and meta-analysis of randomized
528 controlled trials. Phytother Res 33:2609-2621.

529 Hoffmann A, Cheng G, Baltimore D (2025) NF-κB: Master regulator of cellular responses in
530 health and disease. Immun Inflamm 1:2.

531 Huang L, Zhao J, Wei Y, Yu G, Li F, Li Q (2021a) Structural characterization and mechanisms
532 of macrophage immunomodulatory activity of a pectic polysaccharide from Cucurbita
533 moschata Duch. Carbohydr Polym 269:118288.

534 Huang L, Zhao J, Wei Y, Yu G, Li Q (2021b) Characterization of a neutral polysaccharide from
535 pumpkin (Cucurbita moschata Duch) with potential immunomodulatory activity. Int J
536 Biol Macromol 188:729-739.

537 Jin W, Zhou H, Zhao H, Pei Y, Su F, Li Y, Luo T (2025) Isolation, in vitro antioxidant capacity,
538 hypoglycemic activity and immunoactivity evaluation of polysaccharides from
539 Coriandrum sativum L. Antioxidants (Basel) 14:149.

Kumar A, Paliwal R, Gulbake A (2023) Lentinan: An unexplored novel biomaterial in drug and gene delivery applications. J Control Release 356:316-336.

Kumar Varma CA, Jayaram Kumar K (2017) Structural, functional and pH sensitive release characteristics of water-soluble polysaccharide from the seeds of Albizia lebbeck L. Carbohydr Polym 175:502-508.

Kwon HY, Choi SI, Han X, Men X, Jang GW, Choi YE, Kim SH, Kang JC, Cho JH, Lee OH (2020) Enhancement of immune activities of mixtures with Sasa quelpaertensis Nakai and Ficus erecta var. sieboldii. Foods 9:868.

Li GL, Tang JF, Tan WL, Zhang T, Zeng D, Zhao S, Ran JH, Li J, Wang YP, Chen DL (2023) The anti-hepatocellular carcinoma effects of polysaccharides from Ganoderma lucidum by regulating macrophage polarization via the MAPK/NF-κB signaling pathway. Food Funct 14:3155-3168.

Li JY, Yi C, Zhu MQ, Yuan YF, Chen G, Qiu NN, Shen L, Song LY, Liu WL, Zhang XL (2025) Immunomodulatory actions of tonifying polysaccharides: Pharmacological effects, mechanisms and therapeutic applications. Front Immunol 16:1640679.

Li M, Huang X, Wen J, Wu X, Ma W, Cui SW, Xie M, Nie S (2022) Comprehensive characterization of glucomannans from different sources to trigger moderate macrophages immune activation. Carbohydr Polym 296:119933.

Li M, Huang X, Wen J, Chen S, Wu X, Ma W, Cui SW, Xie M, Nie S (2023) Innate immune receptors co-recognition of polysaccharides initiates multi-pathway synergistic immune response. Carbohydr Polym 305:120533.

Li SZ, Shu QP, Zhou HM, Liu YY, Fan MQ, Liang XY, Qi LZ, He YN, Liu XY, Du XH, Huang XC, Chen YZ, Du RL, Liang YX, Zhang XD (2024) CLK2 mediates IκBα-independent early termination of NF-κB activation by inducing cytoplasmic redistribution and degradation. Nat Commun 15:3901.

Liao B, Zheng J, Xia C, Chen X, Xu Q, Duan B (2023) The potential, challenges, and prospects of the genus Spirulina polysaccharides as future multipurpose biomacromolecules. Int J

567 Biol Macromol 253:127482.

568 Liu N, Dong Z, Zhu X, Xu H, Zhao Z (2018) Characterization and protective effect of
569 Polygonatum sibiricum polysaccharide against cyclophosphamide-induced
570 immunosuppression in Balb/c mice. Int J Biol Macromol 107:796-802.

571 Liu T, Zhang L, Joo D, Sun SC (2017) NF-κB signaling in inflammation. Signal Transduct
572 Target Ther 2:17023.

573 Liu Z, Liu Z, Li L, Zhang J, Zhao Q, Lin N, Zhong W, Jiang M (2022) Immunomodulatory
574 effects of the polysaccharide from Sinonovacula constricta on RAW264.7 macrophage
575 cells. Food Sci Nutr 10:1093-1102.

576 Lundberg JO, Weitzberg E (2022) Nitric oxide signaling in health and disease. Cell 185:2853-
577 2878.

578 Mao H, Zhao X, Sun SC (2025) NF-κB in inflammation and cancer. Cell Mol Immunol 22:811-
579 839.

580 Marjanović B, Benković M, Jurina T, Sokač Cvetnić T, Valinger D, Gajdoš Kljusurić J, Jurinjak
581 Tušek A (2024) Bioactive compounds from Spirulina spp.—Nutritional value, extraction,
582 and application in food industry. Separations 11:257.

583 Mussbacher M, Derler M, Basílio J, Schmid JA (2023) NF-κB in monocytes and
584 macrophages—An inflammatory master regulator in multitalented immune cells. Front
585 Immunol 14:1134661.

586 Niu MM, Guo HX, Shang JC, Meng XC (2023) Structural characterization and
587 immunomodulatory activity of a mannose-rich polysaccharide isolated from
588 Bifidobacterium breve H4-2. J Agric Food Chem 71:19791-19803.

589 Oeckinghaus A, Hayden MS, Ghosh S (2011) Crosstalk in NF-κB signaling pathways. Nat
590 Immunol 12:695-708.

591 Park MD, Silvin A, Ginhoux F, Merad M (2022) Macrophages in health and disease. Cell
592 185:4259-4279.

593 Patel AK, Vadrale AP, Singhania RR, Michaud P, Pandey A, Chen SJ, Chen CW, Dong CD

(2023) Algal polysaccharides: Current status and future prospects. Phytochem Rev 22:1167-1196.

Podgórska-Kryszczuk I (2024) Spirulina—An invaluable source of macro- and micronutrients with broad biological activity and application potential. Molecules 29:5387.

Popko K, Górska E, Stokłosa A, Pływaczewski R, Górecka D, Popko M, Szwed T, Śliwiński P, Wąsik M, Demkow U (2010) The influence of IL-6 and TNF-α genes promoter region polymorphisms (G174C-IL-6 and G308A-TNF-α) on the level of cytokines in obese and normal weight subjects. Cent Eur J Immunol 35:31-36.

Rankin LC, Artis D (2018) Beyond host defense: Emerging functions of the immune system in regulating complex tissue physiology. Cell 173:554-567.

Ricciotti E, FitzGerald GA (2011) Prostaglandins and inflammation. Arterioscler Thromb Vasc Biol 31:986-1000.

Rivera A, Siracusa MC, Yap GS, Gause WC (2016) Innate cell communication kick-starts pathogen-specific immunity. Nat Immunol 17:356-363.

Satitmanwiwat S, Ratanakhanokchai K, Laohakunjit N, Chao LK, Chen ST, Pason P, Tachaapaikoon C, Kyu KL (2012) Improved purity and immunostimulatory activity of β-(1→3)(1→6)-glucan from Pleurotus sajor-caju using cell wall-degrading enzymes. J Agric Food Chem 60:5423-5430.

Shang W, Wang M, Tian F, Wei G, Zhou M, Yan B, Lai C, Huang C, Yong Q (2026) Natural mannose-containing glycans as gut modulators: A mechanistic and translational perspective. Trends Food Sci Technol 172:105709.

Soares MP, Teixeira L, Moita LF (2017) Disease tolerance and immunity in host protection against infection. Nat Rev Immunol 17:83-96.

Song L, Wang S, Fang T, Qiu X, Wang X, Zhou X, Morse MA, Hobeika A, Wu W, Yang H, Ren J, Lyerly HK (2021) Changes in peripheral blood regulatory T cells and IL-6 and IL-10 levels predict response of pediatric medulloblastoma and germ cell tumors with residual or disseminated disease to craniospinal irradiation. Int J Radiat Oncol Biol Phys

111:479-490.

Spínola MP, Mendes AR, Prates JAM (2024) Chemical composition, bioactivities, and applications of Spirulina (Limnospira platensis) in food, feed, and medicine. Foods 13:3656.

Tabarsa M, Dabaghian EH, You S, Yelithao K, Cao R, Rezaei M, Alboofetileh M, Bita S (2020) The activation of NF-κB and MAPKs signaling pathways of RAW264.7 murine macrophages and natural killer cells by fucoidan from Nizamuddinia zanardinii. Int J Biol Macromol 148:56-67.

Wang S, Chen X, Li Q, Zhang Y, Rong Y, Feng Y, Liu H, Xu J, Yang R, Li W (2024) Comparative study on the mechanism of macrophage activation induced by polysaccharides from fresh and dried longan. Nutrients 16:1654.

Wang X, Liu L, Zhang X, Xie D, Hu H, Wang S, Wang D, Wang T (2024) The polysaccharide from Aralia continentalis Kitagawa enhances immune responses via activating the MAPKs and NF-κB signaling pathways in RAW 264.7 macrophages. Chem Biol Technol Agric 11:145.

Wang Y, Wang L, Zhang H, Ren P, Cheng X, Hong F, Liu J, Zhang R, Zhao J, Gou D (2025) Immunostimulatory effects mechanism of polysaccharide extracted from Acanthopanax senticosus on RAW 264.7 cells through activating the TLR/MAPK/NF-κB signaling pathway. Sci Rep 15:13440.

Wang Z, Sun Y, Luo M, He N, Wen Z, Wang Z, Zhang Y, Zhao J, Liu Y (2026) Prostaglandins: Key players in immunomodulation of the nervous system. Neural Regen Res 21:4076-4088.

Wu J, Mo J, Xiang W, Shi X, Guo L, Li Y, Bao Y, Zheng L (2023) Immunoregulatory effects of Tetrastigma hemsleyanum polysaccharide via TLR4-mediated NF-κB and MAPK signaling pathways in Raw264.7 macrophages. Biomed Pharmacother 161:114471.

Wu X, Liu Z, Liu Y, Yang Y, Shi F, Cheong KL, Teng B (2020) Immunostimulatory effects of polysaccharides from Spirulina platensis in vivo and vitro and their activation mechanism

on RAW246.7 macrophages. Mar Drugs 18:538.

Xiang W, Xu L, Zheng L, Zhang QA, Shi X (2024) Purification, structural characterization, and immunoregulatory activity of a polysaccharide from mulberry branch. Chem Biol Technol Agric 11:39.

Xie Y, Wang L, Sun H, Wang Y, Yang Z, Zhang G, Jiang S, Yang W (2019) Polysaccharide from alfalfa activates RAW 264.7 macrophages through MAPK and NF-κB signaling pathways. Int J Biol Macromol 126:960-968.

Xu J, Xiao C, Xu H, Yang S, Chen Z, Wang H, Zheng B, Mao B, Wu X (2021) Anti-inflammatory effects of Ganoderma lucidum sterols via attenuation of the p38 MAPK and NF-κB pathways in LPS-induced RAW 264.7 macrophages. Food Chem Toxicol 150:112073.

Yang F, Li X, Yang Y, Ayivi-Tosuh SM, Wang F, Li H, Wang G (2019) A polysaccharide isolated from the fruits of Physalis alkekengi L. induces RAW264.7 macrophages activation via TLR2 and TLR4-mediated MAPK and NF-κB signaling pathways. Int J Biol Macromol 140:895-906.

Yang S, Zhao M, Jia S (2023) Macrophage: Key player in the pathogenesis of autoimmune diseases. Front Immunol 14:1080310.

Yi S, Xie X, Yu X, Tang M, Toan DT, Yu M, Cao M, Hu T (2025) Arthrospira platensis polysaccharide alleviates inflammation induced by PRV in RAW264.7 cells and mice via the regulation of LncRNA Dhx35/mmu-miR-185-3p/IL-17RA. Algal Res 90:104259.

Yin M, Zhang Y, Li H (2019) Advances in research on immunoregulation of macrophages by plant polysaccharides. Front Immunol 10:145.

Yu Y, Shen M, Song Q, Xie J (2018) Biological activities and pharmaceutical applications of polysaccharide from natural resources: A review. Carbohydr Polym 183:91-101.

Zhang H, Zou P, Zhao H, Qiu J, Regenstein JM, Yang X (2021) Isolation, purification, structure and antioxidant activity of polysaccharide from pinecones of Pinus koraiensis. Carbohydr Polym 251:117078.

675 Zheng Z, Huang Q (2022) New insight into the structure-dependent two-way
676 immunomodulatory effects of water-soluble yeast β-glucan in macrophages. Carbohydr
677 Polym 291:119569.ns in RAW264.7 cells